ISSN 2354-9114 (online), ISSN 0024-9521 (print)
Indonesian Journal of Geography Vol 57, No.1 (2025): 137-145
DOI: : 10.22146/ijg.95745 website: https://jurnal.ugm.ac.id/ijg

INDONESIAN JOURNAL OF GEOGRAPHY

RESEARCH ARTICLE

Geochemical Weathering of Volcanic Materials at Southern Catena of Mount Merapi

Lis Noer Aini[1*)] and Eko Hanudin[2)]

[1)]Faculty of Agriculture, Universitas Muhammadiyah Yogyakarta, Yogyakarta, Indonesia
[2)]Faculty of Agriculture, Universitas Gadjah Mada, Yogyakarta, Indonesia

Received: 2024-04-26
Revised: 2024-06-21
Accepted: 2025-02-25
Published: 2025-04-28

Key words: Catena; geomorphological units; Mount Merapi; total element; weathering index; XRF

Abstract. Soil fertility is enhanced by eruptions of Mount Merapi, which deposits pyroclastic debris rich in weatherable primary minerals. Therefore, this study aimed to assess the geochemical weathering index of soils in the southern catena of Mount Merapi, an area affected by the 2010 eruption. Soil samples were collected to describe 4 geomorphic units, namely the higher, middle, lower, and foot slopes. X-ray fluorescence (X-RF) was conducted to determine total element content, and five weathering indexes (Weathering Index of Parker (WIP), Vogt's Residual Index (V), Chemical Index of Alteration (CIA), Chemical Index of Weathering (CIW), and Plagioclase Index of Alteration (PIA)) were calculated. The results show that aluminum (Al) was the most abundant oxide, followed by calcium (Ca), potassium (K), magnesium (Mg), and sodium (Na). Weathering indexes suggested moderate weathering (WIP > 100, V > 1) with a significant presence of fresh volcanic material (CIA, CIW, PIA between 50-100, closer to 50). Variations in each horizon signified the vertical and horizontal movement of mobile elements. The C horizon (deeper layer) had a higher WIP but lower values for the other indexes. In conclusion, geomorphological units influenced the distribution of fresh volcanic material, weathering products, and translocation of elements. Weathering index values reflected the ongoing release of nutrients from minerals. This information was crucial for developing nutrient management strategies in the Merapi region.

Correspondent email : nenny@umy.ac.id

1. Introduction

Volcanic deposits are formed when magma cools during explosive eruptions (Houghton, 2015). These deposits have diverse physical properties, ranging from fine ash particles to boulder-sized fragments (Brown & Calder, 2005). Volcanic ash, which consists of particles smaller than 2 mm in diameter, is commonly present in both active and inactive volcanoes, with thicknesses ranging from 2.5 cm to 10 cm (Cashman & Rust, 2016) (Anda & Sarwani, 2012). For example, the 2010 eruption of Mount Merapi produced an estimated 1.5×10^8 m^3 of volcanic deposits, while Mount Sinabung's deposits reached approximately 3×10^8 m^3, with thicknesses varying from less than 10 m to 20 m (Pallister et al., 2018). Indonesia contains approximately 129 active volcanoes, accounting for more than 30% of the world's total (Bemmelem, 1970). Mount Merapi, classified as a Type II stratovolcano, has moderate values for radius, slope, and surface roughness at 8.8 km, 15.2°, and 47.7, respectively. Its composition is predominantly intermediate, with a low content of mafic minerals and a high concentration of hydrous minerals. The volcano is also characterized by abundant pumice and lava domes (Suhendro & Haryono, 2023). Frequent eruptions of Indonesia's numerous volcanoes contribute significantly to the accumulation of volcanic deposits. The composition of volcanic ash varies depending on the chemical properties of the source magma (Djobo et al., 2016) For instance, the volcanic ash from Mount Merapi contains 61.55% SiO_2 and 15.85% Al_2O_3. These variations influence the physical and chemical behavior of volcanic deposits, affecting their impact on the environment and potential applications.

Mount Merapi, located in the north of Yogyakarta Special Region (DIY) Province, has a short eruption cycle of 2-6 years, leading to a staged and layered soil formation process (Eko Hanudin, 2011; Pusat Vulkanologi dan Mitigasi Bencana Geologi, 2011). The composition of volcanic ash depends on the chemistry of the source magma (Djobo, 2016). Most volcanic ashes primarily contain silica and alumina, which present pozzolanic activity (Siddique, 2012). Previous studies showed that Merapi volcanic material had mineral content dominated by volcanic glass (60%) and Labradorite (34%). Its chemical composition includes Al (1.8 - 5.9%), Mg (1 - 2.4%), Si (2.6 - 28%), Fe (1.4 - 9.3), SiO_2 (45.70%), Fe_2O_3 (18.20%), CaO (16.10%), Al_2O_3 (14%), and K_2O (3.86%) (Fiantis et al., 2009; Kusumastuti, 2012; Sudaryo, 2009). Anda & Sarwani (2012) stated that the volcanic ash content of the 2010 Merapi eruption was dominated by 49% volcanic glass, 26% labradorite, and 13% augite. Meanwhile, Aini et al. (2019) reported that the material content of Merapi includes 50% volcanic glass, 30% plagioclase, 10% Hornblende, 6% quartz, and 4% opaque. The mineral content and geochemical composition of volcanic material influence vegetation succession.

There are 3 weathering processes that play an important role in soil formation. These include physical (mechanical), chemical, and biological weathering, which occur

simultaneously. The rate of weathering is influenced by internal factors such as mineral composition and geochemistry, as well as external properties, namely climate, topographic position, and organisms. The physical process caused by water, wind, and temperature, leads to cracks or breaks without altering chemical composition. The chemical process includes oxidation, hydrolysis, and carbonation, while the biological counterpart is caused by the activity of plant roots or animal life. Soil is a very complex open system where the formation is driven by weathering of the parent material which takes place together with pedogenetic processes due to abiotic and biotic factors (Sirbu-Radasanu et al., 2022).

As an active volcano, Merapi has a unique landscape that can be classified into five units, namely volcanic cone, slope, foot, foot plain, and fluvio volcanic foot plain (Santosa & Sutikno, 2006; Sutikno et al., 2020). The landform is an interaction between the type of material and geomorphic processes (Aini et al., 2018). The weathering process contributes to nutrient availability for plants, while organic matter and climatic conditions further accelerate material breakdown. Several factors influence rock weathering, particularly temperature, and rainfall, which can reach various depths of the pedosphere, depending on material characteristics, hydrological conditions, and biota activity (Buggle et al., 2011; Mello et al., 2022; Perri, 2020). This process transforms primary minerals into secondary, accompanied by the release of nutrients in the rock. Protons (H+) derived from carbonic acid and organic acids produced by micro-macro-organisms play a crucial role in dissolving elements in volcanic materials. The order of element release typically follows valence levels, starting from monovalent, divalent, and trivalent elements. The balance between the three groups of elements is used to calculate the weathering index value based on the percentage of oxide forms. Additionally, the results of Aini et al. (2019) showed that the potential for Ca, Mg, P, and K nutrients in the Merapi area was quite high.

To assess weathering in the southern catena of Mount Merapi, it is essential to measure the weathering index of volcanic material, which influences the recovery rate of the area. Therefore, this study aimed to examine the weathering process in the southern catena of Mount Merapi through various methods.

2. Methods

Study Area

Sampling was conducted using a stratified approach based on the distribution of geomorphic units in the southern catena of Mount Merapi, as detailed in Figure 1. Samples were collected from areas affected by the 2010 Merapi eruption and characterized into 4 geomorphic units, namely upper (S1 and S2), middle (S3 and S4), lower (S5 and S6), and foot slopes (S7 and S8).

Soil Sampling and Analysis

Soil sampling was conducted at 8 representative points corresponding to 4 geomorphological units, namely upper, middle, lower, and foot slopes. Samples were collected by making a soil profile measuring 2 m x 1 m x 2 m based on the formation of soil horizons. The total nutrient content was determined using XRF analysis, which was performed at Tambakbayan Yogyakarta National Research and Innovation Agency. Not all samples from each horizon in the 8 representative profiles were used in the analysis of soil samples. Considering efficiency, a representative horizon A, B, and C was selected to describe the vertical and horizontal distribution of aluminum (Al), calcium (Ca), magnesium (Mg), potassium (K), and sodium (Na).

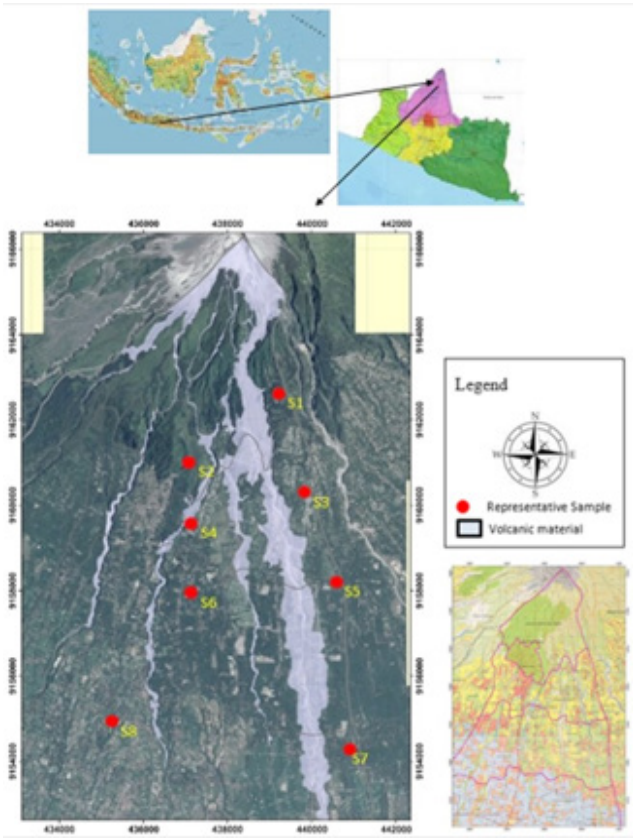

Figure 1. The location of soil samples taken represents each geomorphological unit

Table 1. Summary of weathering indexes

Index	Formula	Optimum Fresh Value	Optimum weathered value
WIP	$[(2Na_2O/0.35)+(MgO/0.9)+(2K_2O/0.25)+(CaO/0.7)] \times 100$	>100	0
V	$(Al_2O_3 + K_2O)/(MgO + CaO + Na_2O)$	>1	Infinite
CIA	$[Al_2O_3/(Al_2O_3 + CaO + Na_2O + K_2O)]x100$	≤ 50	100
CIW	$[Al2O3/(Al_2O_3 + CaO + Na_2O)]x100$	≤ 50	100
PIA	$[(Al_2O_3 - K_2O)/(Al_2O_3 + CaO + Na_2O - K_2O)]x100$	≤ 50	100

Reference: Fiantis et al. (2010)

Methods of Interpreting Rock Weathering

The soil weathering process was assessed by calculating the weathering index. Soil samples were prepared in wind-dry conditions and passed through a 0.5 mm sieve. Weathering was evaluated using 5 methods, namely Weathering Index of Parker (WIP), Vogt's Residual Index (V), Chemical Index of Alteration (CIA), Chemical Index of Weathering (CIW), and Plagioclase Index of Alteration (PIA), with the formulas presented in Table 1.

3. Result and Discussion

Eruption History of Mount Merapi to Volcanic Material Distribution

Mount Merapi is a well-documented example of a highly active volcano, with eruptions occurring at intervals of 2-6 years (Ratdomopurbo and Poupinet, 2000). These events are typically dominated by pyroclastic flows, a consequence of lava dome collapse (Hidayati et al., 2008). Surono et al. (2012) identified a distinct eruption type with a significantly longer recurrence interval of 50-100 years. The larger eruptions were more explosive and had a higher magnitude, as exemplified by the 2010 event. This cyclical behavior emphasized Merapi's long active history, with over 80 eruptions documented since 1006 (source needed). The persistent activity has earned Merapi the nickname of "a never-sleep volcano." The eruptive style oscillated between explosive and effusive phases. Explosive eruptions generated pyroclastic flows, while effusive phases produced lava domes and flows. The domes can collapse, triggering the characteristic "*nuee ardente d'avalanche Merapi type*" pyroclastic flows (source needed). The prevailing direction of these eruptions tended to be westward or southwestward, as documented by various studies (Andreastuti et al., 2006; Sudradjat et al., 2010; Putra et al., 2011; Sudibyakto, 2011a).

As an active stratovolcano, Mount Merapi had unique landforms that originated from the interplay of diverse materials and dynamic geomorphic processes. These landforms significantly influenced soil types and groundwater characteristics (Summerfield, 1991; Brown, 1995; Gerrard, 1995). The topography significantly impacted the velocity and volume of deposited volcanic material. Regions proximate to the eruption source or frequently traversed by lava flows developed distinct soil morphologies. Frequent deposition of new material in these areas caused polygenesis, leading to complex soil profiles.

Field observation showed that the upper and middle slopes had a mountainous topography and were hilly, respectively. Meanwhile, the lower and foot slopes featured an undulating landscape and flat terrain. These conditions influenced weathering processes and soil formation. The rate of rock was affected by several factors, including topography, climate, physical characteristics of rocks, chemical characteristics and rock structures, as well as vegetation. Climatic conditions characterized by high rainfall and high temperatures accelerate the process.

Morphological and Climatological Conditions of the Study Area

Mount Merapi, situated approximately 32 km north of Yogyakarta, Indonesia, is located close to the center of Java Island. The study area, comprising the southern catena of Mount Merapi, is geographically positioned between 7°32'5"S and 110°26'5"E. The elevation in this region ranged from 447 to 1197 meters above sea level, with slopes varying between gentle (0-3%) and extremely steep (>40%).

Monthly precipitation in the study area typically falls between 15,35 and 456,20 mm. The rainfall distribution, as shown in Figure 2, had a dry season from July to September. Consequently, the moisture regime was identified as "udic" due to the duration of the dry season being less than 90 cumulative days (Soil Survey Staff, 2014).

Following the methodology of Schmidt and Ferguson (1951), the Q value presented in Table 1 was adopted to assess the moisture regime. This value represents the percentage difference between the average rainfall of the driest and wettest months. Months with average rainfall below 60 mm, between 60 and 100 mm, and exceeding 100 mm were classified as dry, moist, and wet, respectively. Based on the classification, the study area with a Q value of 0,475 was categorized as "C type" (rather wet).

Based on data from the Meteorology and Geophysics (BMG) climatology station, during the past 10 years (2015-2024) the average value of the lowest and highest temperatures reached ±23^{O}C and ±32^{O}C, respectively, as detailed in Figure 3. Therefore, the temperature regime could be categorized as isohyperthermic due to the mean annual soil record of 22°C (Soil Survey Staff, 2014).

High rainfall and warm temperatures are the main characteristics of the monsoon climate in tropical areas. These conditions supported the weathering process in the area to run relatively quickly compared to subtropical and other climates.

Geochemical Characteristics of Soil at the Southern Catena of Mount Merapi

The rate of rock weathering was influenced by two factors, namely the physical-chemical-mineralogical properties of the rock and external conditions originating from the role of biotic (flora and fauna) and abiotic (climate and topography)

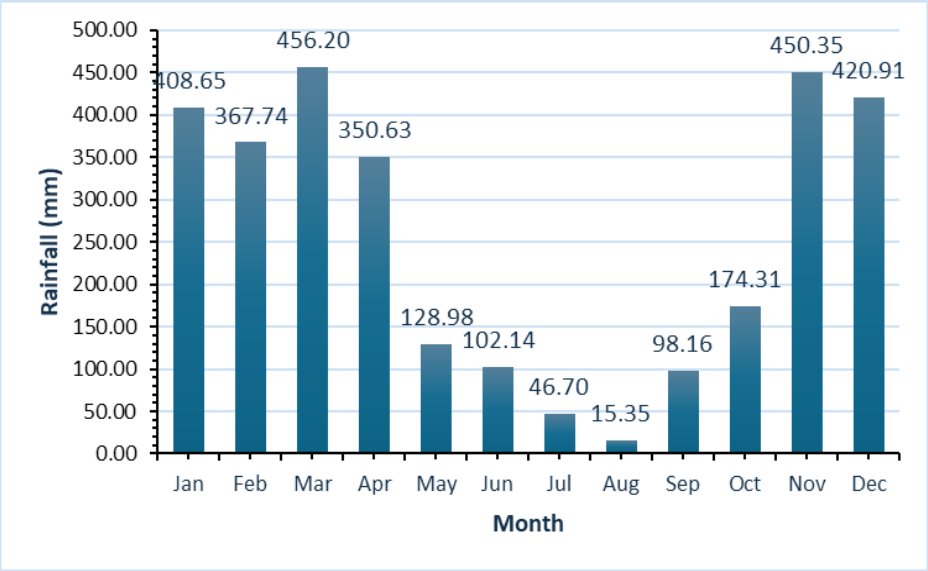

Figure 2. The distribution of rainfall in the study area

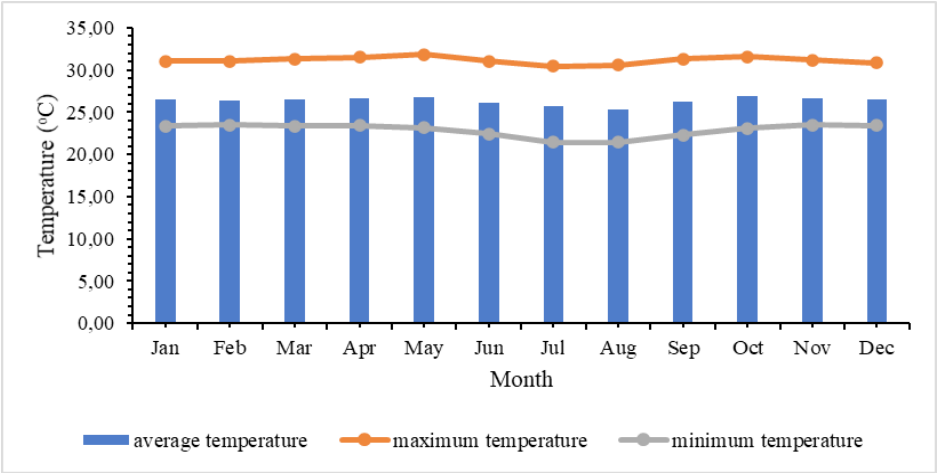

Figure 3. Temperature variability during 2015-2024 (10 years) in study area

elements. The total elemental content in the southern catena of Mount Merapi, which served as a determinant of the weathering process is presented in Table 3. Field observation of soil profiles in this region showed polygenesis, identified in samples 1, 2, 3, and 4. Soil in areas with a mountainous topography, polygenesis often occurs due to climate variations, erosion, and geomorphic conditions that shape the landscape (Waroszewski et al., 2018).

Geochemical composition characterization of soil samples was conducted using X-ray fluorescence (X-RF) technology, a new method in soil analysis. The development of technology in the field of X-rays is increasingly sophisticated to facilitate application in various fields. Advances in technology based on the principles of physics also affect methods in soil chemical analysis, specifically for total elements. Previous methods used many chemical principles, namely strong acids such as HNO3, HClO4, HCl, and H2O2. This method which is often known as Wet digestion, enhances the efficiency of digestion through acid mixtures (Hödrejärv and Vaarmann, 1999). In Indonesia, a mixture of HNO_3 + $HClO_4$ is usually used with a ratio of 3: 1 (SRI, 2009). In America, Lim and Jackson (1982) adopted HCl + HNO_3 with a ratio of 3: 1 which was later known as aquaregia solution. Melo and Guedes (2020) also used the same extractor for soil analysis in Brazil. In Canada, Sheldrick (1984) applied HNO_3+$HClO_4$+HF at a ratio of 1:1:1 for the analysis of total nutrient levels in soil. In the limitations of wet destruction, not all elements can be dissolved, specifically Si which precipitate in highly acidic conditions. This precipitation prevents accurate measurement using a UV-VIS spectrophotometer or Atomic Absorption Spectrophotometer (AAS). Due to the inability to achieve complete decomposition, Oeztan and Duering (2011) referred to wet digestion as pseudo-total analysis (PTA). The same opinion has also been expressed by Hödrejärv and Vaarmann (1999).

XRF spectroscopy is a powerful analytical method that rapidly determines the total concentration of elements in solid and liquid samples (Weindorf & Chakraborty, 2020). The method offers significant advantages (pun intended) compared to traditional wet-chemistry methods, particularly in the ability to analyze unprepared solid samples, eliminating the need for harsh chemicals and lengthy preparation steps (Gredilla et al., 2016; Marguí, 2022). This translates to faster analysis times and minimal environmental impact, corresponding perfectly with the principles of green chemistry.

The application of XRF for soil analysis presents a transformative approach to assessing nutrient content in agricultural settings (Rossel & Bouma, 2016). Traditional methods often required extensive sample preparation and potentially hazardous chemicals, while XRF provided a rapid, field-portable option for on-site analysis (Ayers & Wallace,

1998). This allows for immediate decision-making regarding fertilizer application and soil amendments, leading to more targeted nutrient management practices (McBridge, 2014).

The distribution of Al, Na, Mg, K and Ca both vertically and horizontally is presented in Table 3 and Figure 2. In general, the element levels from highest to lowest were sorted as Al>Ca>K>Mg and Na. The S1 profile, located in the upper slope area, shows the presence of polygenesis. This implied that one Pedon has two soil profiles with the same great group name, such as Typic Hapludand (Aini et al., 2018). In most cases, the levels of these five elements increase towards deeper depths, approaching the parent material. As an exception, the CaO level in the A1 horizon was higher than the underlying horizon. This is possibly due to the addition of new material from volcanic activity. Meanwhile, in the 2A2 horizon, the levels of Al, Na, K, and Ca were higher than in the 2B2, possibly due to elemental enrichment from the upper horizon by the percolation water. Profile S1 and S2 showed a similar trend with the Pedon featuring only one profile (monogenesis).

In the middle slope geomorphological unit represented by profiles S3 and S4, the total element content in horizon C was higher than in horizons A and B. This is expected since horizon C consists of parent material, formed through weathering of fresh rock. In other horizons, the levels are lower, possibly due to leaching. Specifically for soils that have more than one profile (polygenesis) characterized by more than 1 C horizon, A horizon below was enriched with elements from the C horizon above due to the vertical translocation process by percolated water. The high and low levels of elements in soil were greatly influenced by mineralogical composition,

Table 3. Elemental content (expressed in oxides) in soil in the southern catena of Mount Merapi

Representative Sample	Horizon	Al_2O_3 (%)	Na_2O (%)	MgO (ppm)	K_2O (%)	CaO (%)
S1	1A	17,18	0,135	0,336	6,07	6,90
	1B	18,21	0,135	0,474	6,34	5,98
	1C	18,39	0,137	0,580	6,39	6,43
	2A2	16,47	0,159	0,344	5,27	6,09
	2B2	15,75	0,118	0,358	4,17	4,98
	2C	19,70	0,168	0,797	4,35	7,37
	C2	18,69	0,150	0,178	6,52	9,15
S2	C	19,34	0,135	0,314	2,49	3,49
	A1	16,47	0,124	0,376	4,76	6,76
	B2	17,17	0,128	0,438	3,90	3,85
	C	17,74	0,099	0,323	6,48	8,58
S3	1B	20,80	0,113	0,350	3,22	4,60
	2A	19,30	0,125	0,553	3,05	4,13
	2C	20,92	0,087	0,331	3,03	4,27
	A2	16,80	0,065	0,214	4,62	6,76
	C2	18,31	0,069	0,277	5,66	9,43
S4	A2	18,27	0,147	0,620	4,05	6,00
	C2	18,76	0,134	0,486	4,98	8,30
	2A	18,47	0,127	0,620	4,57	7,07
	2B	18,50	0,123	0,556	4,44	6,81
S5	1A	19,13	0,120	0,327	3,11	4,59
	1B	17,58	0,107	0,346	3,48	4,49
	1C	17,62	0,109	0,386	4,97	7,44
	A1	19,14	0,094	0,298	4,40	5,99
	B	20,23	0,080	0,503	3,04	4,93
	C2	19,33	0,084	0,285	4,42	6,10
S6	A	17,37	0,138	0,608	4,66	7,66
	B	18,80	0,168	0,643	4,64	7,60
	BC2	18,29	0,183	0,551	4,95	9,13
	C4	17,73	0,173	0,424	6,20	8,98
S7	(C)	18,76	5,97	0,281	5,97	9,19
	A2	18,36	2,85	0,328	2,85	5,42
	A3	17,88	2,23	0,274	2,23	4,88
	A4	18,37	2,04	0,231	2,04	4,62
S8	A1	16,32	4,20	0,287	5,97	6,77
	B1	16,68	3,72	0,316	2,85	6,15
	C2	18,40	4,14	0,211	2,23	6,41

topographic position, population and types of organisms, rainfall intensity, and air temperature. The total element levels of these two profiles were sequentially from highest to lowest, namely Al>Ca>K>Mg>Na.

In the lower slope unit area, represented by profiles S5 and S6, the levels of Al, Na, Mg, K, and Ca had a similar trend to the profile on the upper and middle slopes. The levels of the five elements in the C horizon were higher than other horizons. In several cases, the levels of these elements in the A horizon were relatively high. This may be attributed to the topographic position, where volcanic material from higher elevations has been translocated and deposited in lower areas. Lower slopes can be classified into a deposition zone, where material translocated from the upper area is deposited.

Profiles S7 and S8 represent soil samples in the foot slope area of the southern catena of Mount Merapi. In the S7 profile, a layer of volcanic material was still present, retaining properties similar to the parent soil material and symbolized by (C). From the analysis results, the total element content remained relatively high. When the layer is overgrown with grass and accumulated organic material, it is categorized as A horizon. The analysis results showed that the levels of the elements Al, Na, Mg, K, and Ca are relatively high. The levels of the five elements are in the order of Al>Ca>K>Mg>Na. This is related to the mineral composition in volcanic materials. The highest were Al and Si, followed by other base cations. Al is a trivalent cation and Ca as a divalent cation was more immobilized than K, Mg, and Na.

When compared between geomorphological units, the highest levels of these five elements were observed in soil profile S6 located on a lower slope. Meanwhile, the lowest content was obtained S3 which was located in the middle slope geomorphic unit, as detailed in Figure 2. The diversity of essential and non-essential nutrient levels in soil shows the important role of geomorphological units in influencing the distribution of fresh volcanic material, weathering products, transformation processes, and translocation of primary mineral constituent elements. The southern catena of Mount Merapi was dominated by the mineral pyroxene, which is easily weathered. This led to the easy release of the elemental content (Aini et al., 2019) as pyroxene contributes to the large amount of Ca contained in the southern catena of Mount Merapi (Massimo Nespolo, 2021)

Rock weathering processes can be assessed by calculating the weathering index, which provides insights into pedogenesis. Several methods are available for determining the weathering index, including the WIP, V, CIA, CIW), and PIA. The weathering index introduced by Parker (Price & Velbel, 2003) evaluates weathering based on the proportion of base cations, which are among the most mobile elements due to their oxygen bonds. V calculates weathering maturity by assessing residual sediment composition. Roaldset (1972) applied this method to determine the weathering status of clays in the Numedal Quaternary deposits in Norway. CIA quantifies the conversion of primary minerals into secondary minerals, such as the transformation of feldspar into kaolinite, and is particularly relevant for laterite-dominated environments (Fiantis et al., 2010). CIW, introduced by Harnois & Moore (1988), follows a similar calculation to CIA but excludes K_2O. It is also based on the alteration of primary minerals into secondary minerals (Fiantis et al., 2010). PIA measures weathering based on the abundance of plagioclase in silicate rocks, given its high solubility (Fedo et al., 1995). The index is particularly useful for monitoring plagioclase weathering.

Table 4. shows the magnitude of the weathering index that occurs based on WIP, V, CIA, CIW, and PIA calculations.

Analysis using the WIP system showed that the highest weathering in the upper slope geomorphic unit occurred in the C horizon, as observed in both S1 and 2. The highest weathering index was recorded in the C horizon at the final stage of the genesis process, while the lowest weathering varied across horizons. In S1, the lowest index appeared in the 2B2 horizon, but in S2, it was recorded in the 1C horizon. The two samples had different parent materials, with S1 and S2 originating from the young and old Merapi formation, respectively. According to weathering index V, the highest weathering in S1 was observed in the 1B horizon. As a B horizon, it had undergone further weathering, resulting in a higher elemental content. In contrast, S2 recorded the highest weathering index in the 1C horizon, a stacked horizon undergoing continuous genesis processes. Calculations using CIA, CIW, and PIA showed that in the S1 profile, the highest index occurred in the 2B2 horizon.

In the middle slope geomorphic unit, the WIP index for the S3 profile was highest and lowest in the C and A horizons, respectively. V index showed the highest weathering in the 2C

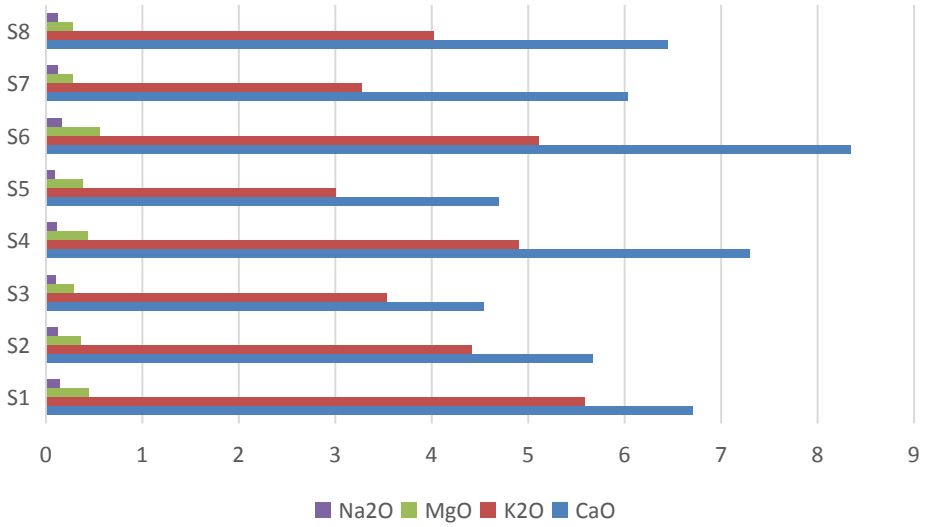

Figure 2. Elemental content in the southern catena of Mount Merapi

Table 4. Weathering index in the southern catena of Mount Merapi

Geomorphic unit	Representative Sample	WIP	V	CIA	CIW	PIA
Upper Slope	S1 - 1A	5959,18	3,15	56,72	70,94	61,21
	S1 - 1B	6053,74	3,72	59,38	74,85	65,98
	S1 - 1C	6172,82	3,47	58,67	73,69	64,63
	S1 - 2A2	5214,11	3,30	58,85	72,49	64,19
	S1 - 2B2	4154,81	3,65	62,95	75,54	69,43
	S1 - 2C	4716,26	2,88	62,36	72,31	67,05
	S1 - C2	6627,47	2,66	54,15	66,76	56,67
	S2 - 1C	2606,76	5,54	75,95	84,20	82,27
	S2 - A1	4888,03	2,93	58,59	70,54	62,99
	S2 - B2	3794,94	4,78	68,55	81,21	76,95
	S2 - C	6500,70	2,69	53,94	67,16	56,49
Middle Slope	S3 - 1B	3338,65	4,74	72,38	81,52	78,85
	S3 - 2A	3165,91	4,65	72,53	81,93	79,24
	S3 - 2C	3122,00	5,11	73,90	82,77	80,42
	S3 - A2	4724,22	3,05	59,48	71,13	64,10
	S3 - C2	5942,57	2,45	54,72	65,85	57,13
	S4 - A2	4247,57	3,30	64,19	74,83	69,83
	S4 - C2	5303,83	2,66	58,30	68,99	62,02
	S4 - 2A	4811,89	2,95	61,07	71,95	65,86
	S4 - 2B	4655,47	3,06	61,92	72,72	66,96
Lower Slope						
	S5 - 1A	3251,13	4,42	70,98	80,25	77,29
	S5 - 1B	3526,44	4,26	68,52	79,29	75,43
	S5 - 1C	5148,22	2,85	58,44	70,00	62,61
	S5 - A1	4459,23	3,69	64,62	75,88	70,79
	S5 - B	3241,46	4,22	71,53	80,15	77,43
	S5 - C2	4489,82	3,67	64,56	75,75	70,67
	S6 - A	4968,38	2,62	58,23	69,01	61,97
	S6 - B	4962,34	2,79	60,25	70,77	64,59
	S6 - BC2	5426,90	2,36	56,19	66,26	58,89
	S6 - C4	6390,70	2,50	53,58	65,94	55,73
Foot Slope	S7 - C	6208,75	2,57	55,06	66,75	57,79
	S7 - A2	3159,19	3,62	68,65	76,85	73,71
	S7 - A3	2567,88	3,83	71,26	78,21	75,86
	S7 - A4	2371,71	4,13	73,11	79,57	77,59
	S8 - A1	4426,97	2,86	59,55	70,32	63,77
	S8 - B1	3968,62	3,09	62,50	72,64	67,34
	S8 - C2	4319,59	3,35	63,31	73,82	68,61

horizon for S3 and A2 horizon for S4, possibly due to differences in microclimate, topography, and material accumulation. CIA, CIW, and PIA calculations also placed the highest weathering in the 2C horizon for S3 and A2 horizon for S4, with both profiles featuring the lowest index in the C2 horizon.

In the lower slope geomorphic units, CIA, CIW, and PIA calculations showed the highest weathering in the 1A horizon of S5 and B horizon of S6. However, WIP calculations identified a 1C horizon for S5 and BC2 for S6. V index was in line with CIA, CIW, and PIA, placing the highest weathering in 1A horizon for S5 and B horizon for S6.

In the foot slope geomorphic unit, WIP calculation showed the highest weathering index in the C horizon in the S7 profile and the A1 horizon in the S8 profile. V calculations presented the highest weathering in the A4 and C2 horizons of the S7 and S8 profiles, respectively. CIA, CIW, and PIA calculations also identified the A4 and C2 horizons of S7 and S8 as the most weathered.

The variability of weathering index across geomorphological units is presented in Figures 3 and 4. V, CIA, CIW, and PIA values are similar across the 4 slope units, reflecting the dominance of young Merapi formations on the southern slop, which limits weathering.

WIP values in Figure 4 vary, with the highest on the upper slope and lower slope. It was important to acknowledge that the lowest values were on middle and foot slopes. The ranking followed the order of upper slope>lower slope>middle slope>foot slope. This suggested WIP was more sensitive to topography than other indexes.

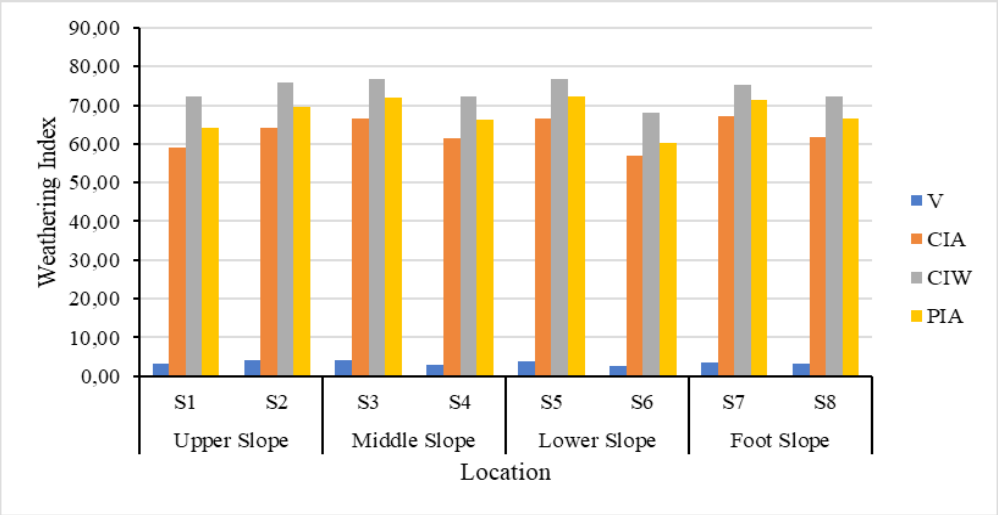

Figure 3. Weathering index of V, CIA, CIW, and PIA at each geomorphological unit

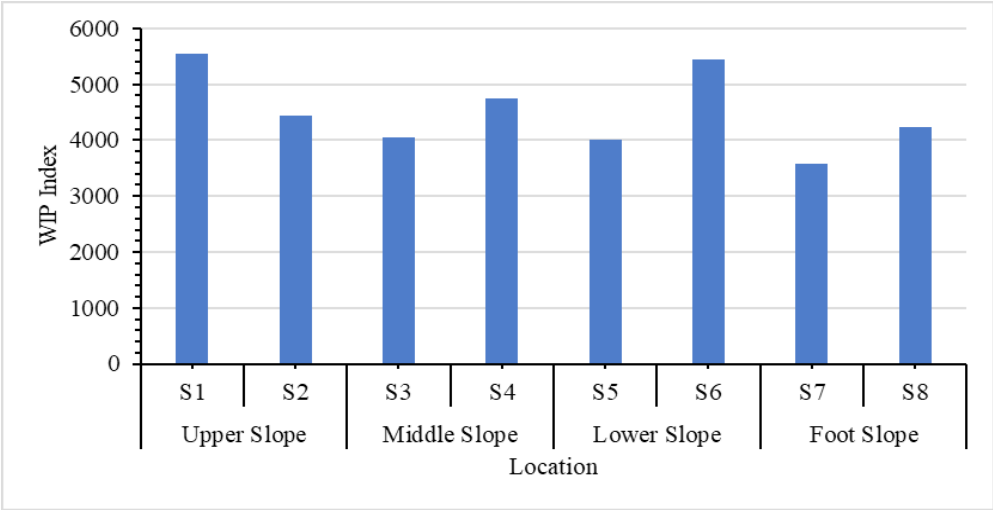

Figure 4. Variability of the WIP index at each geomorphological unit

Weathering index calculations showed differences in the horizons affected by weathering, depending on the method used. Fiantis et al. (2010) stated that WIP was suitable for determining the base mobility of volcanic materials, with higher values signifying more extensive weathering. In contrast, CIA, CIW, and PIA calculations focus on plagioclase weathering.

Aini et al. (2019) showed that the southern slope of Mount Merapi was dominated by plagioclase, causing weathering indexes based on CIA, CIW, and PIA to occur on the same horizon. Plagioclase is a primary mineral that contains many elements of Ca, Mg, and Na. The microclimatic conditions and vegetation cover are different, leading to different weathering horizons in each geomorphic unit.

4. Conclusion

In conclusion, the results showed that the levels of oxides followed the order Al>Ca>K>Mg>Na. Based on the data on the levels of these oxides, the value of the weathering index is calculated. WIP values > 100, V > 1, while CIA, CIW, and PIA values ranged between 50 and 100. This signified that volcanic material had begun to weather, and the fresh material content remained high, as the values were close to 50. Variations in the inter-horizon weathering index suggested the translocation of basic cations such as Ca, Mg, K, and Na both vertically and horizontally. WIP value in the C horizon tended to be higher than in other horizons, while the other 4 indexes showed the opposite trend. The diversity of essential and non-essential nutrient levels in soil emphasized the important role of geomorphological units in influencing the distribution of fresh volcanic material, weathering products, transformation processes, and translocation of primary mineral constituent elements. The high levels of weatherable minerals in this volcanic material played a crucial role in determining nutrient management strategies in the Merapi area.

Acknowledgment

The authors are grateful to the Directorate General of Higher Education for providing funding through the Basic Research Grant Scheme for Higher Education Excellence in 2021.

References

Andreastuti, S, D., Newhall, C., and Dwiyanto, J (2006). Menelusuri Kebenaran Letusan Gunung Merapi 1006. Jurnal Geologi Indonesia. Vol. 1, No 4, pp. 201-207.

Aini, L. N., Soenarminto, B. H., Hanudin, E., & Sartohadi, J. (2019). Plant nutritional potency of recent volcanic materials from the southern flank of mt. Merapi, Indonesia. *Bulgarian Journal of Agricultural Science*, *25*(3), 527–533.

Aini, L. N., Sunarminto, B. H., Hanudin, E., & Sartohadi, J. (2018). Soil morphogenesis diversity at the southern flank of Merapi Volcano, Indonesia five years post-eruption. *Indian Journal of Agricultural Research*, *52*(of), 472–480. https://doi.org/10.18805/IJARe.A-325

Anda, M., & Sarwani, M. (2012). Mineralogy, Chemical Composition, and Dissolution of Fresh Ash Eruption: New Potential Source of Nutrients Article. *Soil Science Society of America Journal*, *76*(January), 733–747. https://doi.org/10.2136/sssaj

Buggle, B., Glaser, B., Hambach, U., Gerasimenko, N., & Marković, S. (2011). An evaluation of geochemical weathering indices in loess–paleosol studies. *Quaternary International*, *240*(1–2), 12–21. https://doi.org/10.1016/j.quaint.2010.07.019

Eko Hanudin. (2011). Pendekatan Agrogeologi Dalam Pemulihan Lahan Pertanian Pasca Erupsi Merapi (Agrogeology Approach in Recovering Agricultural Land after Merapi Volcano Eruption) Volcano Eruption). *Prosiding Seminar Nasional HITI "Upaya Pemulihan Lahan Akibat Erupsi Gunungapi,"* 1–15.

Fedo, C. M., Wayne Nesbitt, H., & Young, G. M. (1995). Unraveling the effects of potassium metasomatism in sedimentary rocks and paleosols, with implications for paleoweathering conditions and provenance. *Geology*, *23*(10), 921. https://doi.org/10.1130/0091-7613(1995)023<0921:UTEOPM>2.3.CO;2

Fiantis, D., Nelson, M., Shamshuddin, J., Goh, T. B., & Van Ranst, E. (2010). Determination of the Geochemical Weathering Indices and Trace Elements Content of New Volcanic Ash Deposits from Mt. Talang (West Sumatra) Indonesia. *Eurasian Soil Science*, *43*(13), 1477–1485. https://doi.org/10.1134/S1064229310130077

Fiantis, D., Nelson, M., Van Ranst, E., Shamshuddin, J., & Qafoku, N. P. (2009). Chemical weathering of new pyroclastic deposits from Mt. Merapi (Java), Indonesia. *Journal of Mountain Science*, *6*(3), 240–254. https://doi.org/10.1007/s11629-009-1041-3

Harnois, L., & Moore, J. M. (1988). Geochemistry and origin of the Ore Chimney Formation, a transported paleoregolith in the Grenville Province of southeastern Ontario, Canada. *Chemical Geology*, *69*(3–4), 267–289. https://doi.org/10.1016/0009-2541(88)90039-3

Kusumastuti, E. (2012). Pemanfaatan abu vulkanik gunung merapi sebagai geopolimer (suatu polimer anorganik aluminosilikat). *Jurnal MIPA Unnes*, *35*(1), 66–76.

Massimo Nespolo. (2021). Encyclopedia of Geology (Second Edition). Pyroxenes. *Academic Press*, *5*, 428–441. https://doi.org/https://doi.org/10.1016/8978-0-12-4095498-9.124091

Mello, D. C. de, Ferreira, T. O., Veloso, G. V., Lana, M. G. de, Mello, F. A. de O., Di Raimo, L. A. D. L., Cabrero, D. R. O., Souza, J. J. L. L. de, Fernandes-Filho, E. I., & Francelino, M. R. (2022). Weathering intensities in tropical soils evaluated by machine learning, clusterization and geophysical sensors. *SOIL Discussions*, *June*, 1–41. https://doi.org/https://doi.org/10.5194/soil-2022-17

Perri, F. (2020). Chemical weathering of crystalline rocks in contrasting climatic conditions using geochemical proxies: An overview. *Palaeogeography, Palaeoclimatology, Palaeoecology*, *556*(October), 109873. https://doi.org/10.1016/j.palaeo.2020.109873

Price, J. R., & Velbel, M. A. (2003). Chemical weathering indices applied to weathering profiles developed on heterogeneous felsic metamorphic parent rocks. *Chemical Geology*, *202*(3–4), 397–416. https://doi.org/10.1016/j.chemgeo.2002.11.001

Pusat Vulkanologi dan Mitigasi Bencana Geologi. (2011). Laporan dan Kajian Vulkanisme Erupsi: Edisi Khusus Erupsi Merapi 2006. In *Acta Universitatis Agriculturae et Silviculturae Mendelianae Brunensis*. https://katalog.kemdikbud.go.id/index.php?p=show_detail&id=95220&keywords=

Roaldset, E. (1972). Mineralogy And Geochemistry of Quaternary Clays In The Numedal Area, Southern Norway. *Norsk Geologisk Tidsskrift*, *52*, 335–369. https://foreninger.uio.no/ngf/ngt/pdfs/NGT_52_4_335-369.pdf

Santosa, L. W., & Sutikno. (2006). Geomorphological Approach for Regional Zoning In The Merapi Volcanic Area. *Indonesian Journal of Geography,* 38(1), 53–68.

Sirbu-Radasanu, D. S., Huzum, R., Dumitraş, D.-G., & Stan, C. O. (2022). Mineralogical and Geochemical Implications of Weathering Processes Responsible for Soil Generation in Mănăila Alpine Area (Tulgheş 3 Unit—Eastern Carpathians). *Minerals*, *12*(9), 1161. https://doi.org/10.3390/min12091161

Sudaryo, S. (2009). Identifikasi Dan Penentuan Logam Pada Tanah Vulkanik Di Daerah Cangkringan Kabupaten Sleman Dengan Metode Analisis Aktivasi Neutron Cepat. *Seminar Nasional V Sdm Teknologi Nuklir Yogyakarta*, 715–718.

Suhendro, I., & Haryono, E. (2023). Typology of Indonesian Stratovolcanoes: Insights from Geomorphological and Geological Aspects. *Indonesian Journal of Geography*, *55*(2), 275–288. https://doi.org/10.22146/ijg.74692

Sutikno, Widiyanto, Santosa, L. W., Kurniawan, A., & HeryPurwanto, T. (2020). Distribution of natural resources and population density in the merapi volcano area. *Indonesian Journal of Geography* 35(2), 55–66. https://doi.org/10.22146/IJG.57270

Waroszewski, J., Egli, M., Brandová, D., Christl, M., Kabala, C., Malkiewicz, M., Kierczak, J., Glina, B., & Jezierski, P. (2018). Identifying slope processes over time and their imprint in soils of medium-high mountains of Central Europe (the Karkonosze Mountains, Poland). *Earth Surface Processes and Landforms*, *43*(6), 1195–1212. https://doi.org/10.1002/esp.4305

Weindorf, D.C.; Chakraborty, S. (2020). Portable X-ray fluorescence spectrometry analysis of soils. Soil Sci. Soc. Am. J. 84: 1384–1392.